Human Molecular Genetics, 2018, Vol. 27, No. 18 3272–3282

doi: 10.1093/hmg/ddy233
Advance Access Publication Date: 20 June 2018
Original Article

ORIGINAL ARTICLE

TNNT1 nemaline myopathy: natural history and therapeutic frontier

Michael D. Fox[1,2,3,†], Vincent J. Carson[1,†], Han-Zhong Feng[4], Michael W. Lawlor[5], John T. Gray[6], Karlla W. Brigatti[1], J.-P. Jin[4] and Kevin A. Strauss[1,*]

[1]Clinic for Special Children, Strasburg, PA, USA, [2]Department of Pediatrics, Sidney Kimmel Medical College at Thomas Jefferson University, Philadelphia, PA, USA, [3]Diagnostic Referral Division, Nemours/Alfred I. duPont Hospital for Children, Wilmington, DE, USA, [4]Department of Physiology, Wayne State University School of Medicine, Detroit, MI, USA, [5]Department of Pathology and Laboratory Medicine and Neuroscience Research Center, The Medical College of Wisconsin, Milwaukee, WI, USA and [6]Audentes Therapeutics, San Francisco, CA, USA

*To whom correspondence should be addressed at: Clinic for Special Children, 535 Bunker Hill Road, Strasburg, PA 17579, USA. Tel: +1 7176879407; Fax: +1 7176879237; Email: kstrauss@clinicforspecialchildren.org

Abstract

We describe the natural history of 'Amish' nemaline myopathy (ANM), an infantile-onset, lethal disease linked to a pathogenic c.505G>T nonsense mutation of *TNNT1*, which encodes the slow fiber isoform of troponin T (TNNT1; a.k.a. TnT). The *TNNT1* c.505G>T allele has a carrier frequency of 6.5% within Old Order Amish settlements of North America. We collected natural history data for 106 ANM patients born between 1923 and 2017. Over the last two decades, mean age of molecular diagnosis was 16 ± 27 days. *TNNT1* c.505G>T homozygotes were normal weight at birth but failed to thrive by age 9 months. Presenting neonatal signs were axial hypotonia, hip and shoulder stiffness, and tremors, followed by progressive muscle weakness, atrophy and contractures. Affected children developed thoracic rigidity, pectus carinatum and restrictive lung disease during infancy, and all succumbed to respiratory failure by 6 years of age (median survival 18 months, range 0.2–66 months). Muscle histology from two affected children showed marked fiber size variation owing to both Type 1 myofiber smallness (hypotrophy) and Type 2 fiber hypertrophy, with evidence of nemaline rods, myofibrillar disarray and vacuolar pathology in both fiber types. The truncated slow TNNT1 (TnT) fragment (p.Glu180Ter) was undetectable in ANM muscle, reflecting its rapid proteolysis and clearance from sarcoplasm. Similar functional and histological phenotypes were observed in other human cohorts and two transgenic murine models (*Tnnt1*$^{-/-}$ and *Tnnt1* c.505G>T). These findings have implications for emerging molecular therapies, including the suitably of *TNNT1* gene replacement for newborns with ANM or other TNNT1-associated myopathies.

Introduction

Biallelic mutations of various sarcomere genes (i.e. *TNNT1, NEB, ACTA1, TPM3, TPM2, MYPN, CFL2, KBTBD13, KLHL40, KLHL41, LMOD3*) cause nemaline rod myopathy (MIM PS161800) (1), first formally described in 1963 and so named for the distinctive electron-dense, rod-like aggregates in sarcoplasm (2–4). Nemaline myopathies are clinically heterogeneous,

[†]The authors wish it to be known that, in their opinion, the first two authors should be regarded as joint First Authors.
Received: March 20, 2018. **Revised:** June 4, 2018. **Accepted:** June 6, 2018

Table 1. Troponin and myosin isoforms in human and murine muscle

Protein isoforms	Human gene symbol	Murine gene symbol	Human/murine protein symbol	Alternative name
Slow skeletal muscle troponin T	*TNNT1*	*Tnnt1*	TNNT1	slow TnT
Slow skeletal muscle troponin I	*TNNI1*	*Tnni1*	TNNI1	slow TnI
Fast skeletal muscle troponin T	*TNNT3*	*Tnnt3*	TNNT3	fast TnT
Fast skeletal muscle troponin I	*TNNI2*	*Tnni2*	TNNI2	fast TnI
Cardiac troponin T	*TNNT2*	*Tnnt2*	TNNT2	Cardiac TnT
Cardiac troponin I	*TNNI3*	*Tnni3*	TNNI3	Cardiac TnI
Skeletal muscle myosin heavy chain type 1	*MYH7*	*Myh7*	MYH7	MHC I
Skeletal muscle myosin heavy chain type 2a	*MYH2*	*Myh2*	MYH2	MHC IIa (2a)
Skeletal muscle myosin heavy chain type 2b	*MYH1*	*Myh1*	MYH1	MHC IIx (2b)

with a phenotypic spectrum that includes variable and progressive muscle weakness, hypoventilation, dysphagia and speech impairment. Intellectual function is characteristically preserved (1,5–10). Collectively, nemaline myopathies represent the most common class of non-dystrophic muscle disease in humans, affecting more than 1 per 50 000 newborns (8,11,12).

The troponin complex (Table 1; Fig. 1) was first linked to nemaline myopathy in the Year 2000, when a pathogenic *TNNT1* c.505G>T nonsense mutation was discovered among six children of common Amish descent who suffered from infantile-onset, lethal myopathy, distinguished by progressive pectus carinatum deformity, known colloquially as 'chicken breast disease' (13). Five additional *TNNT1* mutations have been associated with a similar recessive phenotype in non-Amish ethnic groups (Table 2, Fig. 1) (9,14–16), and one *TNNT1* variant (c.311A>T; p.Glu104Val) was recently linked to dominant myopathy among 10 subjects related across 4 generations (10). Thus, TNNT1 myopathies are of increasing medical relevance; they can now be diagnosed in at least 29 laboratories worldwide and have been incorporated into 44 different next-generation sequencing panels (Genetic Testing Registry, March 2018; https://www.ncbi.nlm.nih.gov/gtr/).

The troponin complex mediates calcium-sensitive interactions between actin and tropomyosin that govern striated muscle contraction. It is composed of tropomyosin binding (TNNT), calcium-sensing (TNNC) and regulatory (TNNI) subunits, each of which exists in muscle fiber-type-specific isoforms (Table 1; Fig. 1) (17). *TNNT1* encodes the TNNT1 subunit of fatigue-resistant type 1 skeletal muscle fibers; its 756–789 nucleotide sequence is highly conserved among vertebrates and expression is restricted to Type 1, slow-twitch skeletal myofibers (18). The *TNNT1* c.505G>T 'founder' mutation in exon 11 causes 'Amish' nemaline myopathy (ANM) by converting a glutamic acid codon to a premature stop codon (p.Glu180Ter), which truncates the 83 C-terminal amino acids and abrogates TNNI, TNNC and tropomyosin binding (Table 2; Fig. 1) (7). The resulting TNNT1 p.Glu180Ter fragment incorporates poorly into myofilaments and is instead rapidly degraded in sarcoplasm as slow fibers stiffen and degenerate (19,20).

At the Clinic for Special Children (CSC), we interrogate the genetic substructure of Anabaptist demes to provide a foundation for early diagnosis and disease prevention, and here lay the groundwork for intervention studies focused on asymptomatic newborns with ANM. To this end, we present a comprehensive natural history of TNNT1 myopathy within the Old Order Amish population, compare these data to other clinical cohorts (9,10), and describe transgenic animal models suitable for pre-clinical studies of gene replacement therapy (1,21,22).

Results

Patients

We collected data about 106 children of Amish ancestry, born between 1923 and 2017, who died in early childhood from myopathic respiratory failure with pectus carinatum deformity (Fig. 2A). Probands derived from 54 families hailing from four different U.S. states: Pennsylvania ($n = 97$), Maryland ($n = 5$), New York ($n = 3$) and Indiana ($n = 1$). Only one child was living at the time of this manuscript preparation, and date of death was known for 87 (82%) of those deceased.

Diagnosis and population genetics

Molecular testing for *TNNT1* c.505G>T began at CSC laboratory in 1998. For 34 (94%) of 36 affected children born during or after this year, we confirmed molecular diagnosis of ANM at16 ± 27 days of life. Two patients born after 1998 did not have molecular testing but diagnosis could be confidently inferred from Old Order Amish ancestry, linkage to known carriers, and the characteristic phenotype; such was also the case for 70 affected individuals born before 1998. The survival curve in Figure 2 includes data from six ANM patients originally described by Johnston *et al.* (13). To date, only the severe ANM phenotype has been associated with *TNNT1* c.505G>T; cascade screening within this large Amish cohort as well as whole exome sequencing data from more than 1000 population-specific control samples have revealed no milder phenotypes associated with *TNNT1* c.505G>T in heterozygous or homozygous state.

Natural history of ANM

Newborns with ANM were normal weight at birth (3.4 ± 0.1 kg, range 3.2–3.6 kg) but 94% had somatic growth failure by age 9 months (Fig. 2B). Delays in gross and adaptive motor function were evident during infancy. Eleven (61%) of the 18 affected children rolled supine to prone at an average of 7.6 ± 1.1 months but all subsequently lost this skill. Only 2 (11%) sat independently, one of whom could stand with assistance for a brief interval. All children learned to grab objects and employ a pincer grasp but lost these abilities as muscle disease progressed. Receptive language and social development were characteristically preserved.

Presenting motor signs during the neonatal period included axial hypotonia, subtle stiffness of hip and shoulder girdles, and tremors of the limbs and chin accompanied by sustained clonus with provocation. Tremors subsided within a few months of life

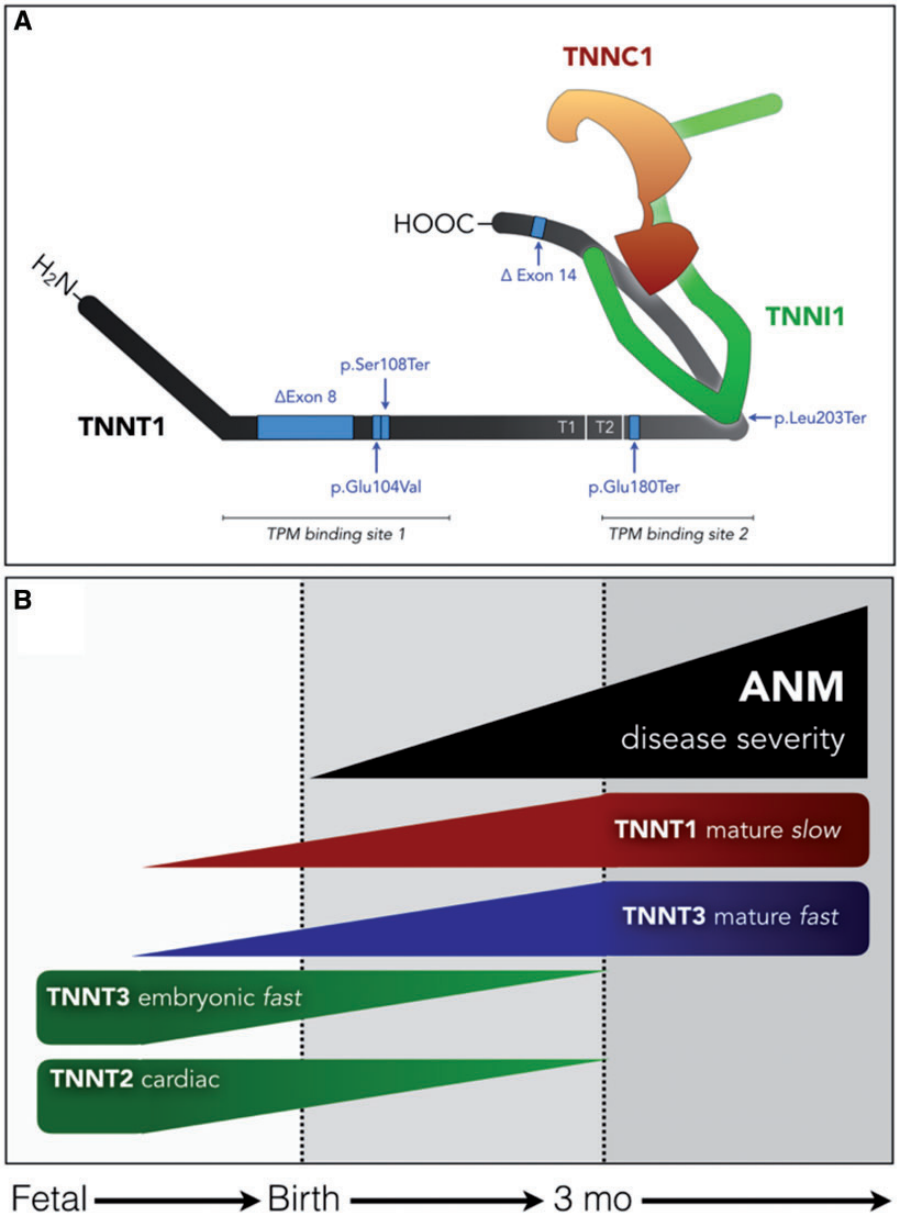

Figure 1. Troponin complex structure, variation, and developmental expression. (**A**) The slow fiber troponin complex is composed of TNNT1 (gray), TNNI1 (green) and TNNC1 (orange) protein subunits. Six pathogenic variants of TNNT1 are indicated by blue arrows (see text and Table 2 for references). The p.Glu180Ter mutation causing Amish nemaline myopathy (ANM) by cleaving the 83 carboxy-terminal amino acids. The residual protein fragment does not bind TNNI1, TNNC1 or tropomyosin, and is rapidly degraded in sarcoplasm. (**B**) During the course of embryological development, immature TNNT isoforms (embryonic TNNT3 and cardiac TNNT2; green) are expressed in skeletal muscle. Beginning around birth and progressing through the first 3–6 months of life, these are replaced by mature TNNT3 (blue) and TNNT1 (red) proteins, closely paralleling the course of muscle weakness and atrophy in children with ANM (black).

as proximal muscles began to develop contracture. By 12 months of age, hip abduction was limited to $<10^{\circ}$ in the majority of affected children (13). Muscle atrophy and weakness progressed in lockstep with contractures, and all children developed a severe pectus carinatum deformity as the thorax became rigid (Fig. 2A). Electromyography performed in two children (ages 14 and 16 months) showed a mild-myopathic pattern with preserved nerve conduction velocity.

Children with ANM suffered from recurrent upper and lower respiratory tract infections (e.g. pneumonia, bronchiolitis and acute otitis media). In all cases, treatment was palliative, delivered exclusively in the home setting and concentrated near the end of life. Only one family used nasogastric feeding and none elected to use invasive or non-invasive ventilatory support. Among 87 (82%) cases for which accurate dates were available, median survival was 18 months (range 0.2–66 months) and 76% of children succumbed to respiratory failure by age 2 years (Fig. 2C). Only one child survived beyond 4 years of age. Over a period of a nearly a century, there was no correlation between date of birth and age of death (Fig. 2D), indicating that Old Order Amish communities are reluctant to use costly or invasive life-sustaining technologies (e.g. tracheostomy, bilevel positive airway pressure, gastrostomy) for children who are otherwise helpless. Thus, we observed the natural history of disease undistorted by technological interventions, hospitalizations or invasive care.

Histology of human TNNT1 myopathy

Fresh muscle biopsies were obtained in August 2017 from two ANM patients, ages 14 and 16 months (Fig. 3) and showed similar pathological findings consistent with severe nemaline rod myopathy. The first specimen (ANM-A; age 14 months, *m. vastus lateralis*) showed marked size variation between discrete subpopulations of small and hypertrophic fibers. The smallest myofibers were generally appropriate in shape, suggesting hypotrophy (insufficient growth) rather than atrophy, and included both Type 1 and Type 2 ATPase fibers. In contrast, hypertrophic fibers were exclusively Type 2 and predominated in the ANM-A specimen (~70% total fibers). We found no definitive evidence of myofiber degeneration, fiber type grouping or inflammation.

Distinctive morphological changes were most conspicuous in a minority of small fibers but were also present to a lesser extent among large fibers. These included (Fig. 3A): (i) central nuclei; (ii) foamy, vacuolated cytoplasm; (iii) basophilic material within cytoplasm (H&E); (iv) granular cytoplasmic inclusions (i.e. nemaline rods); (iv) subsarcolemmal red material suspicious for mitochondrial aggregates (Gomori trichrome); and (v) inappropriately distributed organelles, including dense accumulations of mitochondria and ring-shaped areas, devoid of mitochondria, coincident with myofibrillar disarray (oxidative stains: NADH, SDH, COX). Some fibers displayed numerous darkly stained circular structures (possibly enlarged mitochondria); these were not the source of cytoplasmic vacuolation, nor did vacuoles overlap with prominent lipid droplets (oil red O stain, not shown) seen in rare fibers.

Ultrastructural examination showed nemaline rods colocalizing with myofibrillar disarray (Fig. 3B). Mitochondria were

Table 2. Monogenic TNNT1 nemaline myopathies

Ethnicity	Protein variant	Inheritance	Reference(s)
Old Order Amish	p.Glu180Ter	AR	Johnston *et al.* (13) and Jin *et al.* (19)
Dutch	ΔExon 8	AR[a]	van der Pol *et al.* (14)
Dutch	ΔExon 14	AR[a]	van der Pol *et al.* (14)
Hispanic	p.Ser108Ter	AR	Marra *et al.* (15)
Palestinian	p.Leu203Ter	AR	Abdulhaq *et al.* (9)
Iranian	p.Leu203Ter	AR	Fattahi *et al.* (16)
Not specified	p.Glu104Val	AD	Konersman *et al.* (10)

[a]Compound heterozygous variants in Dutch kindred.
AD, autosomal dominant; AR, autosomal recessive.

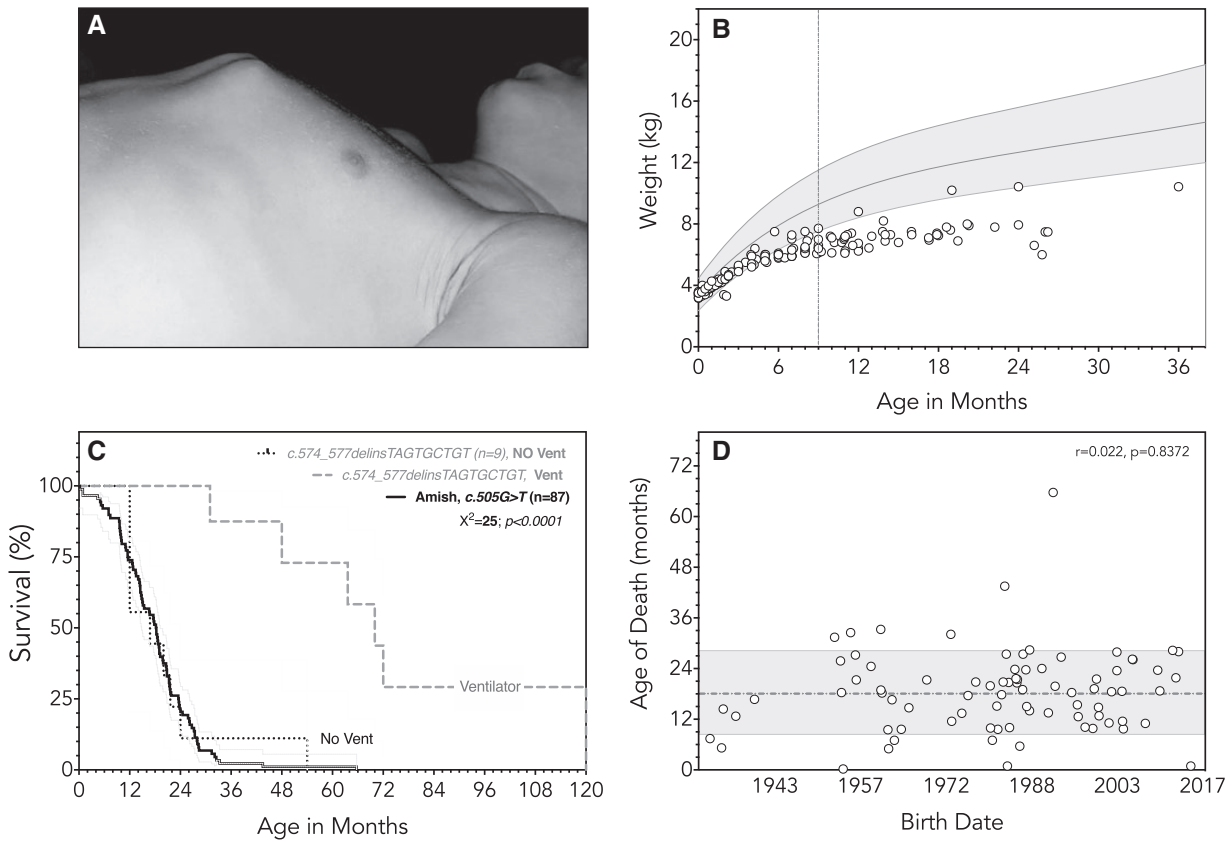

Figure 2. Natural History of ANM. (**A**) Progressive contracture of intercostal muscles causes a characteristic deformity of the developing thorax and sternochondral joints. (**B**) Newborns with ANM (open circles) are normal weight at birth (3.4 ± 0.1 kg, range 3.2–3.6 kg) but have somatic growth failure by age 9 months (dotted line; gray shaded area represents World Health Organization reference curves for females, 3rd to 97th centiles). (**C**) Age of death was accurately known for 87 of 105 ANM patients (solid line); median survival was 18 months (range 0.2–66 months). Also shown for comparison are survival data for nine Palestinian children homozygous for a different *TNNT1* variant (c.574_577delinsTAGTGCTGT) [data redrawn from Abdulhaq *et al.* (9)]. The dashed line shows longer absolute median survival of 70 months for this cohort (chi square=25, $P < 0.0001$). However, if ventilator dependence is taken as a proxy for death, median 'ventilator-free' survival for Amish (solid line) and Palestinian (dotted line) children with recessive TNNT1 myopathy were nearly identical. (**D**) Between 1923 and 2017, age of death (open circles) was unrelated to date of birth for children with ANM (Pearson's $r = 0.022$, $P = 0.8372$), indicating a lack of disease-modifying therapies and the reluctance of Old Order Amish families to utilize invasive, life-sustaining measures for an otherwise fatal disease.

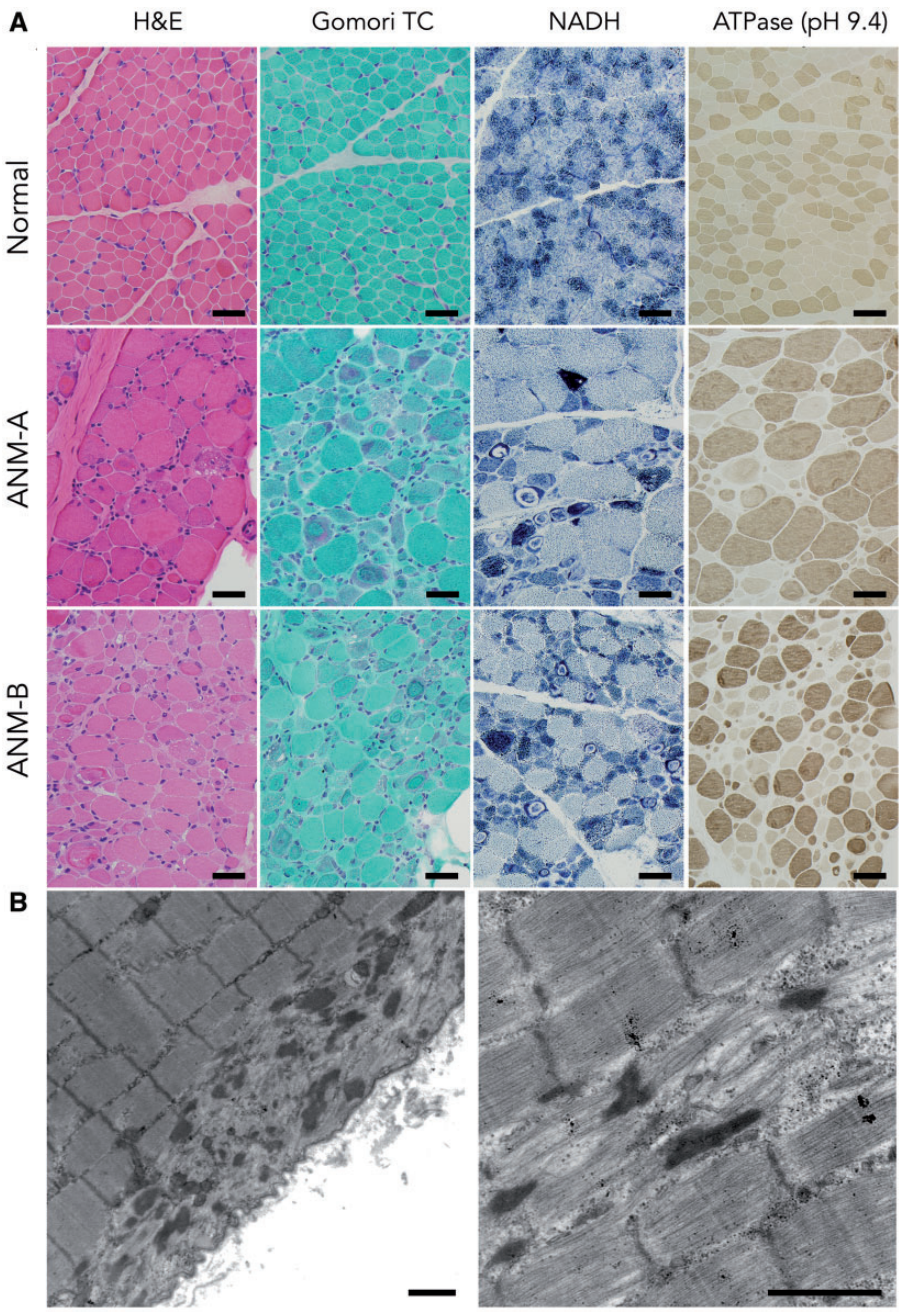

Figure 3. Histological Findings in Human ANM. (**A**) In comparison to a normal muscle biopsy from the *m. vastus lateralis* muscle of a 17-month-old boy (upper panels), muscle biopsies from two ANM patients (ANM-A, middle panels; and ANM-B, lower panels) display marked abnormalities of myofiber size (both hypotrophy and hypertrophy) and increased numbers of internally nucleated fibers on hematoxylin and eosin (H&E) staining. Some fibers show areas of vacuolization. Gomori trichrome stain highlights aggregates of granular reddish-purple inclusions (nemaline rods), along with ring-like subsarcolemmal areas of myofibrillar disorganization. NADH stain (which highlights mitochondria and elements of the sarcotubular system) shows dense aggregates of these organelles in some fibers as well as areas of clearance within some of the ring-like subsarcolemmal inclusions. An ATPase stain at pH 9.4 (which causes fast type 2 fibers to stain dark brown and slow type 1 fibers to stain light tan) reveals a hypertrophic fiber population exclusively composed of Type 2 fast fibers amid a hypotrophic population of both fiber types (Bar=40 μm). (B) Ultrastructural appearance of nemaline rods (left panel) and myofibrillar disarray (right panel) in ANM muscle (Bar=1 μm).

generally normal in morphology and number, and formed small aggregates in subsarcolemmal regions. Some fibers contained punctate accumulations of glycogen and mitochondria in the intermyofibrillar space that might correspond to vacuolated regions observed by light microscopy. In areas with appropriate myofibrillar organization, the sarcotubular apparatus appeared normal.

Using a combination of western blot and immunohistochemistry (Fig. 4), we found that ANM muscle had absent TNNT1, decreased slow skeletal TNNI1 and increased cardiac TNNT2 (a.k.a. cardiac TnT) (Fig. 4A and B). There was a selective decrease of Type 1 slow fiber content (as indicated by reduced slow skeletal fiber myosin, MYH7; Fig. 4B and C) accompanied by a modest increase of fast skeletal fiber myosin type 2a

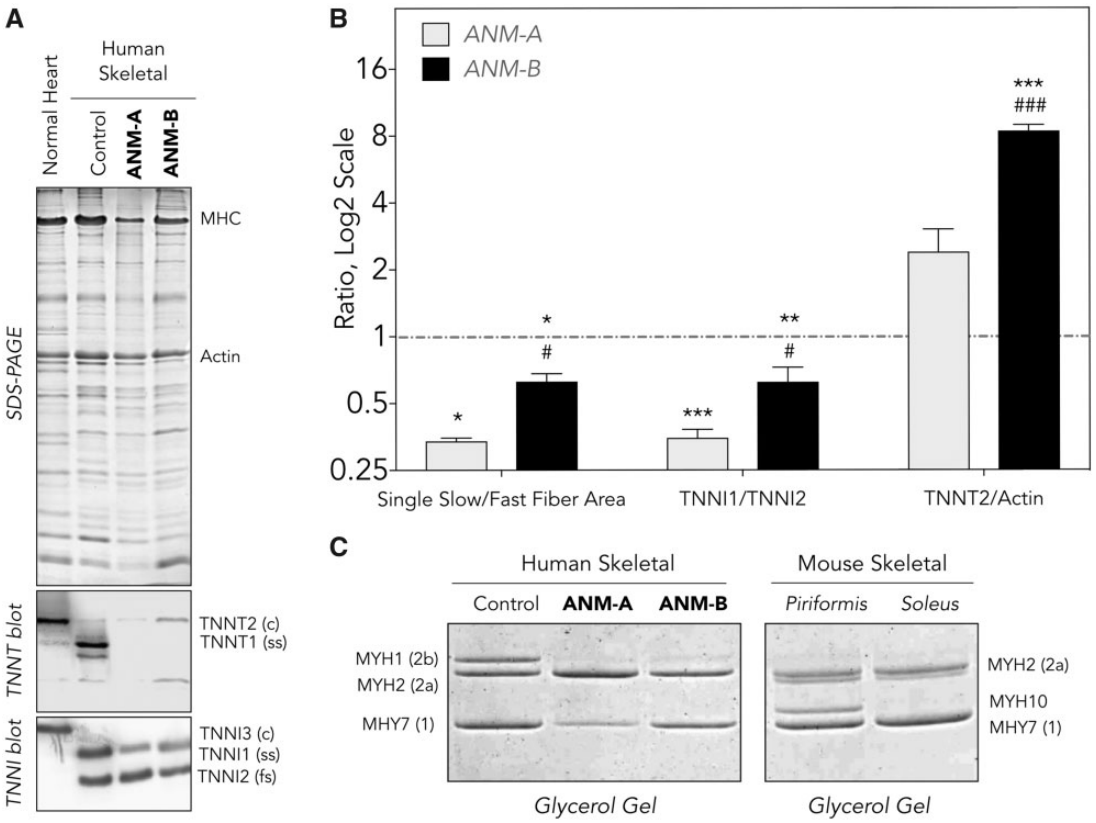

Figure 4. Protein Expression in ANM muscle. (**A**) SDS-gel and western blot of total protein extracts from frozen muscle sections reveals complete loss of TNNT1 (slow skeletal TnT) in *TNNT1* c.505G>T homozygous children ages 14 (ANM-A) and 16 (ANM-B) months. The expression of slow TNNI1 (TnI) is decreased, indicating an overall reduction of slow fiber content. Significant expression of cardiac TNNT2 (cardiac TnT) was detectable, reflecting adaptive muscle regeneration. (**B**) Densitometry analysis of the western blots normalized to protein inputs quantified in parallel SDS-gel confirmed that, relative to normal muscle control tissue (red dashed line), ANM muscles (gray shaded and solid bars) has a 2- to 3-fold lower ratio of slow to fast fibers and slow TNNI1 to fast TNNI2, as well as more abundant cardiac TNNT2, as sign of adaptive muscle regeneration. (**C**) Relative to human control muscle, *TNNT1* c.505G>T homozygotes had decreased MYH7 (Type 1 myosin) whereas MHY2 (skeletal muscle myosin type 2a) was modestly increased and MHY1 (skeletal muscle myosin type 2b) drastically decreased. These are compared with protein expression in normal murine skeletal muscle. Values are presented as mean±SE. $N = 4$–10 sections of ANM-A or ANM-B muscle. $^{**}P < 0.01$ and $^{***}P < 0.001$ versus WT; $^{\#}P < 0.05$ and $^{\#\#\#}P < 0.001$ versus ANM-A using Student's *t* test. ANM, Amish nemaline myopathy; c, cardiac isoform; fs, fast skeletal isoform; ss, slow skeletal isoform.

(MYH2), such that the ratio of slow (Type 1) to fast (Type 2) fibers in ANM muscle was reduced 2- to 3-fold (Fig. 4B).

The second muscle specimen (ANM-B; age 16 months, *m. rectus femoris*) was similar to the first, with a few notable exceptions: vacuolar pathology was more apparent, the degree of myofiber hypertrophy less striking, and there was a greater burden of nemaline rods. There was an approximately even distribution of Type 1 and 2 fibers in the ANM-B specimen, and again hypertrophic fibers were exclusively Type 2.

Murine Tnnt1 myopathy

Muscle of both *Tnnt1*$^{-/-}$ and *Tnnt1* c.505G>T homozygous mice resembled human ANM tissue (Fig. 5A), showing the absence of TNNT1, marked atrophy/hypotrophy of small type 1 myofibers, apparently adaptive hypertrophy of fast type 2 fibers, and refractile (nemaline) rods (7,17,20). As with human ANM, overt myonecrosis, fiber type grouping and inflammation were notably absent.

Muscle force generation and exercise recovery were impaired in *Tnnt1*$^{-/-}$ and *Tnnt1* c.505G>T homozygous mice. Figure 5B depicts *ex vivo* functional measurement of whole soleus muscles during intermittent muscle fatigue contractions, which shows more rapid and severe loss of force in *Tnnt1*$^{-/-}$ when compared with wild-type muscle, as well as slower and less complete recovery from fatigue.

Discussion

Population genetics of ANM

Old Order Amish communities descended from a small group of Swiss-German Anabaptists and now comprise ~320 000 individuals living in 502 demes throughout North America (23). Shaped by an 18th century population bottleneck and subsequent genetic drift (24), the *TNNT1* c.505G>T carrier frequency among contemporary Amish settlements has equilibrated at a value of 6.5% (1 per 16 individuals), which is the highest observed among any ethnic group (Table 2) and corresponds to a disease incidence of 1 per 960 births.

Prior to 1998, the year we started testing for *TNNT1* c.505G>T at the CSC laboratory, the diagnosis of ANM was assigned to symptomatic infants based on their family history, clinical presentation, disease course and, in five cases, muscle pathology. Genetic testing for the ANM variant has since eliminated

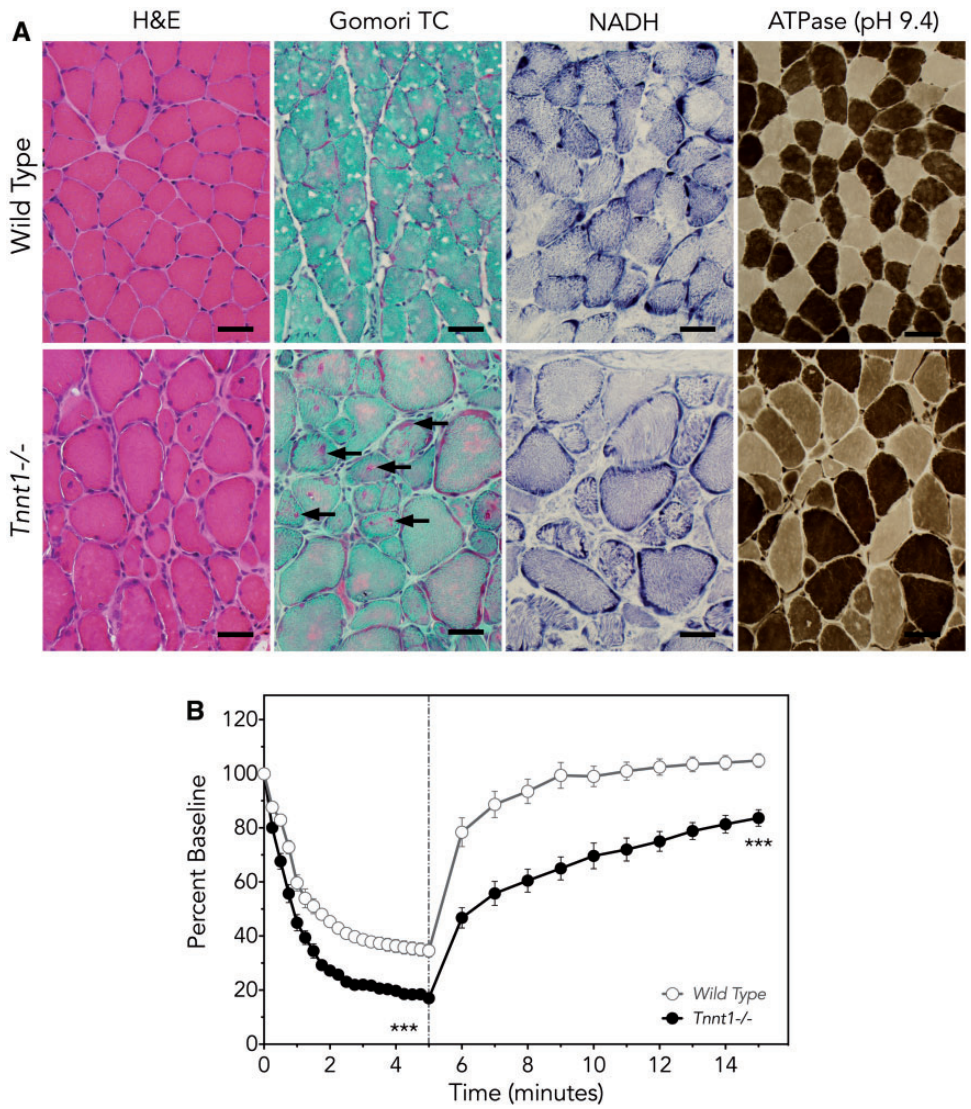

Figure 5. Muscle phenotype of *Tnnt1*$^{-/-}$ mice. (**A**) Compared with control mice (upper panels), *quadratus femoris* muscles from *Tnnt1*$^{-/-}$ (lower panels) mice have myofiber hypertrophy and hypotrophy and internal nucleation similar to that seen in humans with ANM (H&E). Gomori trichrome staining highlights the characteristic granular red nemaline rod aggregates (arrows). In contrast to findings seen in ANM patients, NADH stain shows appropriate distribution of organelles in *Tnnt1*$^{-/-}$ muscle. On ATPase staining (pH 9.4), large and small fiber populations include both slow and fast myofibers, another finding distinct from human ANM muscle (Bar=40 μm), in which hypertrophic fibers are exclusively Type 2. (B) *Ex vivo* functional measurement of whole soleus muscles demonstrates larger and faster loss of force during intermittent muscle fatigue contractions in *Tnnt1*$^{-/-}$ (solid circles) relative to wild-type (open circles) mice. When fatigue contractions terminate (dashed line), *Tnnt1*$^{-/-}$ muscles show slower and less complete recovery from fatigue (*Tnnt1*$^{-/-}$, $n=3$; WT, $n=5$; values as mean±SE, comparison of means, $^{***}P<0.001$ by two-way ANOVA with Bonferroni correction).

diagnostic uncertainty and the need for invasive testing but has not engendered better outcomes over the last century (Fig. 2D). Here we present a comprehensive overview of the ANM phenotype and, by drawing parallels to other human cohorts and transgenic murine models, conclude that TNNT1-linked myopathies are optimal targets for emerging adeno-associated viral (AAV)-based gene replacement strategies (21,25).

The TNNT1 myopathy disease spectrum

Conservative Anabaptists share core beliefs that influence their decisions about end-of-life care (26). As a consequence, Amish parents uniformly rejected inpatient hospitalization, gastrostomy feeding and mechanical ventilation for their children with ANM. We thus observed the natural history of ANM undistorted by life-sustaining technologies. Under these conditions, muscle atrophy and proximal stiffness progressed rapidly over the first year of life and culminated in death between 0.2 and 66 months of age from a combination of respiratory muscle weakness and asphyxiating thoracic deformity.

In 2016, Abdulhaq *et al.* described a similar phenotype among nine Palestinian children homozygous for a different *TNNT1* variant (c.574_577delinsTAGTGCTGT) (9). Affected individuals had transient neonatal jaw and limb tremors and, by 3–4 months of age, developed rapidly progressive proximal weakness, rigidity and limb contractures. Like Amish children with ANM, only 2 (22%) of 9 *TNNT1* c.574_577delinsTAGTGCTGT sat independently. Unlike ANM patients, however, 7 (78%)

Palestinian children were fed by gastrostomy and all started ventilatory support at a median age of 17 (range 12–54) months. Figure 2C shows the striking effect this had on survival; when dependence on mechanical ventilation is taken as a proxy for death, median 'ventilator-free' survival for *TNNT1* c.574_577delinsTAGTGCTGT homozygotes decreases from 70 to 17 months, a value almost identical to that observed for ANM (Fig. 2C).

Muscle tissue from 7 *TNNT1* c.574_577delinsTAGTGCTGT homozygotes showed pathological elements similar to ANM, including Type 1 fiber smallness, Type 2 fiber hypertrophy and the presence of nemaline rods (Fig. 3). These core structural characteristics were first described in a hypotonic infants as early as 1958 (3) and recognized as part of a distinctive congenital myopathy syndrome in 1963 (4). They have now been observed in a variety of muscle specimens from humans (2–4,7,10,13,27), dogs (28), cats (29–31), and two different transgenic murine models (Fig. 5), and appear to be a signature feature of TNNT1-linked myopathies both within and between species.

Until recently, TNNT1 myopathy was considered as a severe autosomal recessive phenotype grouped with other major congenital myopathies (12). However, in 2017 Konersman *et al.* described a later onset form of proximal myopathy segregating in a dominant fashion among 10 related individuals within a large multigeneration pedigree (10,27,32). All affected patients were heterozygous for a *TNNT1* c.311A>T variant that traced back four generations to a common ancestral Ashkenazi Jewish couple. Among affected individuals, proximal weakness was evident between 5 and 20 years of age and followed a slowly progressive course, later accompanied by variable signs such as slender habitus (67%), myopathic-elongated facies (67%), pectus carinatum (33%) and mild kyphoscoliosis (22%). Muscle biopsies showed characteristic fiber type disproportion and nemaline rods.

Although a mild elevation of serum creatine kinase (CK; 249 IU/L) was observed in one *TNNT1* c.311A>T heterozygote, CK levels are generally normal in patients with both dominant and recessive forms of TNNT1 troponin myopathy. Electromyography tracings, reported both here and elsewhere (9,10), show a mild-myopathic pattern ($n = 6$) or appear normal ($n = 3$).

Pathophysiology of troponin myopathy

During muscle contraction, calcium-induced conformational changes of the troponin complex and tropomyosin allow cross-bridges to form between F-actin and myosin, which in turn activates myosin ATPase to generate the power stroke and contractile force (20). Troponin T—via its allosteric interactions with troponin C, troponin I and tropomyosin (Fig. 1)—is central to this process (17,20). Higher vertebrates have three troponin T isoforms corresponding to slow skeletal (TNNT1), fast skeletal (TNNT3) and cardiac (TNNT2) muscle fiber types (Table 1) (18). Most human muscles contain a mix of slow and fast fibers and, accordingly, express both TNNT1 and TNNT3 in a pattern that aligns closely with fiber type distribution (19,33).

The nonsense mutation (*TNNT1* c.505G>T) underlying ANM deletes 83 C-terminal amino acids of TNNT1, eliminates TNNC and TNNI binding sites, and greatly reduces the binding affinity for tropomyosin (Fig. 1A) (17,19). Interestingly, mutant *TNNT1* c.505G>T mRNA is robustly translated in *Escherichia coli* and non-muscle eukaryotic cells to produce truncated TNNT1 p.Glu180Ter at high levels, whereas TNNT1 p.Glu180Ter is absent from ANM muscle despite intact transcription and mRNA processing of the mutant allele (20). The absolute dependence of human muscle on TNNT1-expressing slow myofibers is reflected by the temporal course of ANM: the decay of muscle mass and power closely parallel the expected time course of mature TNNT1 expression in healthy muscle tissue (Fig. 1B).

In ANM muscle, the absence of TNNT1 protein is accompanied by myofiber smallness affecting both the slow and fast fiber populations, but only Type 2 fast fibers are capable of undergoing compensatory hypertrophy. Consistent with the absence of clinical symptoms in *TNNT1* c.505G>T heterozygotes, this observation indicates that muscle cells have a mechanism for rapid proteolysis of truncated TNNT1 p.Glu180Ter (20). Slow troponin I (TNNI1; Fig. 4A) and Type I myosin (MHY7; Fig. 4C) are expressed in ANM muscle. This suggests preservation of viable Type 1 muscle fibers that could be fully restored by introducing wild-type TNNT1 into slow fiber sarcoplasm at an expression level sufficient to keep pace with stoichiometric demands of the contractile machinery.

Therapeutic frontier

The advent of effective myotropic gene vectors (21,22) coincident with presymptomatic diagnostic strategies (34) has reframed the prospect for treating ANM and other TNNT1 myopathies. Among potential carriers and high-risk newborns, we use high-resolution melt analysis to expedite testing for *TNNT1* c.505G>T within 1–2 days of life. As a consequence, most *TNNT1* c.505G>T homozygotes have a confirmed molecular diagnosis prior to the onset of muscle weakness and rigidity, opening a critical window for disease-modifying and potentially life-saving therapies.

Multiple pre-clinical studies underscore the potential to treat human myopathies with AAV vectors (21,35–39), which are small enough to penetrate muscle tissue and for some serotypes exhibit natural myotropism to achieve sustained centrosomal protein expression in post-mitotic myofibrils. In recent studies of murine and canine X-linked centronuclear (a.k.a. myotubular) myopathy (CNMX; MIM 310400), a single intravenous (i.v.) administration of AAV8 vector provided sustained sarcoplasmic expression of myotubularin, decisively prevented muscle degeneration and had minimal toxicity (21,22). Interim data from a Phase I/II study in four boys with CNMX show significant improvements in neuromuscular function, respiratory muscle strength and motor milestone acquisition (https://www.prnewswire.com/) after one i.v. dose of AAV8 vector. Features shared between ANM and CNMX indicate the potential for AAV-based treatment of TNNT1 myopathies (Table 3), including the small size of the gene coding sequence, apparent viability of target muscle cells and the absence of disease-associated immune inflammation (e.g. as has been observed in a subgroup of patients with Duchenne muscular dystrophy) (40).

Many genetic disorders are unsuitable for current gene therapy methods because of progressive tissue pathology secondary to the genetic deficiency, an inability to diagnose the condition prior to onset of irreversible tissue injury, or the lack of available gene delivery vectors that meet packaging requirements and adequately transduce all relevant target tissues. In contrast, ANM is paradigmatic: the pathophysiology appears to arise from a single, myofiber-selective deficiency of TNNT1, encoded by a gene that is ideally sized (1.2 kb) for inclusion into AAV vector particles (Table 3) (25,41). These factors argue strongly for the development of AAV vectors for the delivery of TNNT1 and their testing in the transgenic Tnnt1 p.Glu180Ter mouse model. The selection of an optimal vector expression cassette and

Table 3. Comparison of Amish nemaline rod (ANM) and X-linked centronuclear (CNMX) myopathies

	ANM	CNMX
Cellular biology		
Gene	*TNNT1*	*MTM1*
Inheritance pattern	Autosomal recessive	X-linked recessive
mRNA size	1239 bases	3452 bases
Protein	Type 1 troponin T	Myotubularin
Expression	Sarcoplasm	Sarcoplasm
Localization	Sarcomere	Multiple locations
Function	Calcium-regulated contraction	3-PI phosphatase
Pathology		
Muscle type	Slow skeletal	Ubiquitous
Fiber type	Slow (Type 1)	Ubiquitous
Myofiber appearance	Atrophy/ hypoplasia	Hypotrophy
Myonecrosis	No	No
Inflammation	No	No
Fiber regeneration	Yes	No
Clinical		
Muscle weakness	Progressive	Birth
Muscle wasting	Progressive	Birth
Survival, mean ±SD (months)	18±10	–

dosing regimen in this model may justify transition of such a product to clinical testing, which would provide significant new hope for the children and families around the world afflicted with TNNT1 myopathies (7,9,10,13–16).

Materials and Methods

Human subjects

We used genealogical records, clinical data and molecular reports to collect information about 106 children of Amish ancestry, born between October 1923 and June 2017, who had the distinctive ANM phenotype. Nine families had affected children ($n = 18$) born within the last two decades and consented in writing to a structured survey that allowed us to collect more granular information about growth, development, muscle histology and morbidity. The study was approved by the Lancaster General Hospital Institutional Review Board and all parents consented in writing to participate.

Muscle biopsies were obtained for research through the coordination of the Congenital Muscle Disease Tissue Repository (CMD-TR) and appropriated for routine histological staining [hematoxylin and eosin (H&E), Gomori trichrome, ATPase, NADH, SDH, COX and oil red O], electron microscopy, western blot and immunohistochemistry with monoclonal antibodies FA2 and CT3 (Supplementary Material, Methods). Monoclonal FA2 recognizes myosin heavy chain of Type 1 fibers (MYH7, a.k.a. MHC I; Table 1) and marks slow skeletal myofibers (42). CT3 binds to both slow skeletal (TNNT1) and cardiac troponin T (TNNT2) (7,43,44) but in tissues of *TNNT1* c.505G>T homozygotes and *Tnnt1*$^{-/-}$ mice (which are devoid of TNNT1), selectively detects cardiac TNNT2.

Transgenic murine models

Targeted gene knockout (*Tnnt1*$^{-/-}$) and site-specific knock-in (*Tnnt1* c.505G>T) mice were generated as previously described (7) and muscle specimens were prepped in a manner similar to human specimens. Contractility of intact isolated *quadratus femoris* muscle was examined in superfused preparations as previously described (Supplementary Material, Methods) (45). Developed twitch and tetanic forces were determined at optimal muscle length that gave the highest twitch force, and calculated by subtracting resting tension from total force. Fatigue resistance was examined using an intermittent fatigue protocol (Supplementary Material, Methods) (45).

Statistical methods

Survival of *TNNT1* c.505G>T homozygotes was studied using Kaplan–Meier curves. Pearson's correlation was used to test the relationship between date of birth and age of death. Western blot data comparing human (wild-type) control to ANM (*TNNT1* c.505G>T homozygous) muscle were analyzed using one-way analysis of variance (ANOVA) with Bonferroni correction and a similar statistical paradigm was used to study muscle fatigue data.

Supplementary Material

Supplementary Material is available at *HMG* online.

Acknowledgements

We acknowledge valuable clinical contributions of Drs Richard Kelley, D. Holmes Morton and Thomas Crawford, who provided clinical care for many children with ANM. We also acknowledge Dr Erik Puffenberger, laboratory director at the Clinic for Special Children, for his valuable insight and expertise. We thank Stacy Cossette of the Congenital Muscle Disease Tissue Repository for her assistance with patient consent on muscle biopsy specimens.

Conflict of Interest statement. M.W.L. receives research support and is a member of scientific advisory boards for Audentes Therapeutics, Solid Biosciences and Ichorion Therapeutics, and also serves as a consultant for Wave Life Sciences. J.T.G. is employed by and holds equity interest in Audentes Therapeutics, and also receives royalty and licensing income from St. Jude Children's Research Hospital for technology developed while an employee of that institution. None of the organizations noted provided direct or indirect funding for this study.

Funding

This work was supported by the National Institute of Arthritis and Musculoskeletal and Skin Diseases (AR048816 to J.P.J.); A Foundation Building Strength (in support of the Congenital Muscle Disease Tissue Repository to M.W.L.); and charitable contributions to the Clinic for Special Children from the Amish and Mennonite communities it serves.

References

1. Malfatti, E. and Romero, N.B. (2016) Nemaline myopathies: state of the art. *Rev. Neurol. (Paris)*, **172**, 614–619.
2. Schnell, C., Kan, A. and North, K.N. (2000) 'An artefact gone awry': identification of the first case of nemaline myopathy by Dr R.D.K. Reye. *Neuromuscul. Disord.*, **10**, 307–312.
3. Greenfield, J.G., Cornman, T. and Shy, G.M. (1958) The prognostic value of the muscle biopsy in the floppy infant. *Brain*, **81**, 461–484.

4. Shy, G.M., Engel, W.K., Somers, J.E. and Wanko, T. (1963) Nemaline myopathy. A new congenital myopathy. *Brain*, **86**, 793–810.
5. Lawlor, M.W., Ottenheijm, C.A., Lehtokari, V.L., Cho, K., Pelin, K., Wallgren-Pettersson, C., Granzier, H. and Beggs, A.H. (2011) Novel mutations in NEB cause abnormal nebulin expression and markedly impaired muscle force generation in severe nemaline myopathy. *Skelet Muscle*, **1**, 23.
6. Li, F., Buck, D., De Winter, J., Kolb, J., Meng, H., Birch, C., Slater, R., Escobar, Y.N., Smith, J.E. III, Yang, L. *et al.* (2015) Nebulin deficiency in adult muscle causes sarcomere defects and muscle-type-dependent changes in trophicity: novel insights in nemaline myopathy. *Hum. Mol. Genet.*, **24**, 5219–5233.
7. Wei, B., Lu, Y. and Jin, J.P. (2014) Deficiency of slow skeletal muscle troponin T causes atrophy of type I slow fibres and decreases tolerance to fatigue. *J. Physiol.*, **592**, 1367–1380.
8. Ryan, M.M., Schnell, C., Strickland, C.D., Shield, L.K., Morgan, G., Iannaccone, S.T., Laing, N.G., Beggs, A.H. and North, K.N. (2001) Nemaline myopathy: a clinical study of 143 cases. *Ann. Neurol.*, **50**, 312–320.
9. Abdulhaq, U.N., Daana, M., Dor, T., Fellig, Y., Eylon, S., Schuelke, M., Shaag, A., Elpeleg, O. and Edvardson, S. (2016) Nemaline body myopathy caused by a novel mutation in troponin T1 (TNNT1). *Muscle Nerve*, **53**, 564–569.
10. Konersman, C.G., Freyermuth, F., Winder, T.L., Lawlor, M.W., Lagier-Tourenne, C. and Patel, S.B. (2017) Novel autosomal dominant TNNT1 mutation causing nemaline myopathy. *Mol. Genet. Genomic Med.*, **5**, 678–691.
11. North, K.N., Laing, N.G. and Wallgren-Pettersson, C. (1997) Nemaline myopathy: current concepts. The ENMC International Consortium and Nemaline Myopathy. *J. Med. Genet.*, **34**, 705–713.
12. Witting, N., Werlauff, U., Duno, M. and Vissing, J. (2017) Phenotypes, genotypes, and prevalence of congenital myopathies older than 5 years in Denmark. *Neurol. Genet.*, **3**, e140.
13. Johnston, J.J., Kelley, R.I., Crawford, T.O., Morton, D.H., Agarwala, R., Koch, T., Schaffer, A.A., Francomano, C.A. and Biesecker, L.G. (2000) A novel nemaline myopathy in the Amish caused by a mutation in troponin T1. *Am. J. Hum. Genet.*, **67**, 814–821.
14. van der Pol, W.L., Leijenaar, J.F., Spliet, W.G., Lavrijsen, S.W., Jansen, N.J., Braun, K.P., Mulder, M., Timmers-Raaijmakers, B., Ratsma, K., Dooijes, D. *et al.* (2014) Nemaline myopathy caused byTNNT1 mutations in a Dutch pedigree. *Mol. Genet. Genomic Med.*, **2**, 134–137.
15. Marra, J.D., Engelstad, K.E., Ankala, A., Tanji, K., Dastgir, J., De Vivo, D.C., Coffee, B. and Chiriboga, C.A. (2015) Identification of a novel nemaline myopathy-causing mutation in the troponin T1 (TNNT1) gene: a case outside of the old order Amish. *Muscle Nerve*, **51**, 767–772.
16. Fattahi, Z., Kalhor, Z., Fadaee, M., Vazehan, R., Parsimehr, E., Abolhassani, A., Beheshtian, M., Zamani, G., Nafissi, S., Nilipour, Y. *et al.* (2017) Improved diagnostic yield of neuromuscular disorders applying clinical exome sequencing in patients arising from a consanguineous population. *Clin. Genet.*, **91**, 386–402.
17. Mondal, A. and Jin, J.P. (2016) Protein structure-function relationship at work: learning from myopathy mutations of the slow skeletal muscle isoform of troponin T. *Front. Physiol.*, **7**, 449.
18. Wei, B. and Jin, J.P. (2016) TNNT1, TNNT2, and TNNT3: isoform genes, regulation, and structure-function relationships. *Gene*, **582**, 1–13.
19. Jin, J.P., Brotto, M.A., Hossain, M.M., Huang, Q.Q., Brotto, L.S., Nosek, T.M., Morton, D.H. and Crawford, T.O. (2003) Truncation by Glu180 nonsense mutation results in complete loss of slow skeletal muscle troponin T in a lethal nemaline myopathy. *J. Biol. Chem.*, **278**, 26159–26165.
20. Wang, X., Huang, Q.Q., Breckenridge, M.T., Chen, A., Crawford, T.O., Morton, D.H. and Jin, J.P. (2005) Cellular fate of truncated slow skeletal muscle troponin T produced by Glu180 nonsense mutation in Amish nemaline myopathy. *J. Biol. Chem.*, **280**, 13241–13249.
21. Mack, D.L., Poulard, K., Goddard, M.A., Latournerie, V., Snyder, J.M., Grange, R.W., Elverman, M.R., Denard, J., Veron, P., Buscara, L. *et al.* (2017) Systemic AAV8-mediated gene therapy drives whole-body correction of myotubular myopathy in dogs. *Mol. Ther.*, **25**, 839–854.
22. Childers, M.K., Joubert, R., Poulard, K., Moal, C., Grange, R.W., Doering, J.A., Lawlor, M.W., Rider, B.E., Jamet, T., Daniele, N. *et al.* (2014) Gene therapy prolongs survival and restores function in murine and canine models of myotubular myopathy. *Sci. Transl. Med.*, **6**, 220ra10.
23. Amish Population. Young Center for Anabaptist and Pietist Studies, Elizabethtown College, http://groups.etown.edu/amishstudies/statistics/population-2017/; date last accessed January 5, 2018.
24. Strauss, K.A. and Puffenberger, E.G. (2009) Genetics, medicine, and the Plain people. *Annu. Rev. Genomics Hum. Genet.*, **10**, 513–536.
25. Wu, Z., Yang, H. and Colosi, P. (2010) Effect of genome size on AAV vector packaging. *Mol. Ther.*, **18**, 80–86.
26. Strauss, K.A., Puffenberger, E.G. and Morton, D.H. (2012) One community's effort to control genetic disease. *Am. J. Public Health*, **102**, 1300–1306.
27. Gonatas, N.K., Shy, G.M. and Godfrey, E.H. (1966) Nemaline myopathy. The origin of nemaline structures. *N. Engl. J. Med.*, **274**, 535–539.
28. Delauche, A.J., Cuddon, P.A., Podell, M., Devoe, K., Powell, H.C. and Shelton, G.D. (1998) Nemaline rods in canine myopathies: 4 case reports and literature review. *J. Vet. Intern. Med.*, **12**, 424–430.
29. Shelton, G.D., Sturges, B.K., Lyons, L.A., Williams, D.C., Aleman, M., Jiang, Y. and Mizisin, A.P. (2007) Myopathy with tubulin-reactive inclusions in two cats. *Acta Neuropathol.*, **114**, 537–542.
30. Kube, S.A., Vernau, K.M., LeCouteur, R.A., Mizisin, A.P. and Shelton, G.D. (2006) Congenital myopathy with abundant nemaline rods in a cat. *Neuromuscul. Disord.*, **16**, 188–191.
31. Cooper, B.J., De Lahunta, A., Gallagher, E.A. and Valentine, B.A. (1986) Nemaline myopathy of cats. *Muscle Nerve*, **9**, 618–625.
32. Spiro, A.J. and Kennedy, C. (1965) Hereditary Occurrence of Nemaline Myopathy. *Arch Neurol*, **13**, 155–159.
33. Baldwin, K.M. and Haddad, F. (2001) Effects of different activity and inactivity paradigms on myosin heavy chain gene expression in striated muscle. *J. Appl. Physiol. (1985)*, **90**, 345–357.
34. Olsen, R.K., Dobrowolski, S.F., Kjeldsen, M., Hougaard, D., Simonsen, H., Gregersen, N. and Andresen, B.S. (2010) High-resolution melting analysis, a simple and effective method for reliable mutation scanning and frequency studies in the ACADVL gene. *J. Inherit. Metab. Dis.*, **33**, 247–260.
35. Elverman, M., Goddard, M.A., Mack, D., Snyder, J.M., Lawlor, M.W., Meng, H., Beggs, A.H., Buj-Bello, A., Poulard, K., Marsh, A.P. *et al.* (2017) Long-term effects of systemic gene therapy in a canine model of myotubular myopathy. *Muscle Nerve*, **56**, 943–953.

36. Gatto, F., Rossi, B., Tarallo, A., Polishchuk, E., Polishchuk, R., Carrella, A., Nusco, E., Alvino, F.G., Iacobellis, F., De Leonibus, E. *et al.* (2017) AAV-mediated transcription factor EB (TFEB) gene delivery ameliorates muscle pathology and function in the murine model of Pompe disease. *Sci. Rep.*, **7**, 15089.
37. Pozsgai, E.R., Griffin, D.A., Heller, K.N., Mendell, J.R. and Rodino-Klapac, L.R. (2017) Systemic AAV-mediated beta-sarcoglycan delivery targeting cardiac and skeletal muscle ameliorates histological and functional deficits in LGMD2E mice. *Mol. Ther.*, **25**, 855–869.
38. Tasfaout, H., Lionello, V.M., Kretz, C., Koebel, P., Messaddeq, N., Bitz, D., Laporte, J. and Cowling, B.S. (2018) Single intramuscular injection of AAV-shRNA reduces DNM2 and prevents myotubular myopathy in mice. *Mol. Ther.*, **26**, 1082–1092.
39. Gicquel, E., Maizonnier, N., Foltz, S.J., Martin, W.J., Bourg, N., Svinartchouk, F., Charton, K., Beedle, A.M. and Richard, I. (2017) AAV-mediated transfer of FKRP shows therapeutic efficacy in a murine model but requires control of gene expression. *Hum. Mol. Genet.*, **26**, 1952–1965.
40. Mendell, J.R., Campbell, K., Rodino-Klapac, L., Sahenk, Z., Shilling, C., Lewis, S., Bowles, D., Gray, S., Li, C., Galloway, G. *et al.* (2010) Dystrophin immunity in Duchenne's muscular dystrophy. *N. Engl. J. Med.*, **363**, 1429–1437.
41. Gray, S.J., Matagne, V., Bachaboina, L., Yadav, S., Ojeda, S.R. and Samulski, R.J. (2011) Preclinical differences of intravascular AAV9 delivery to neurons and glia: a comparative study of adult mice and nonhuman primates. *Mol. Ther.*, **19**, 1058–1069.
42. Jin, J.P., Malik, M.L. and Lin, J.J. (1990) Monoclonal antibodies against cardiac myosin heavy chain. *Hybridoma*, **9**, 597–608.
43. Jin, J.P., Yang, F.W., Yu, Z.B., Ruse, C.I., Bond, M. and Chen, A. (2001) The highly conserved COOH terminus of troponin I forms a Ca^{2+}-modulated allosteric domain in the troponin complex. *Biochemistry*, **40**, 2623–2631.
44. Jin, J.P., Chen, A., Ogut, O. and Huang, Q.Q. (2000) Conformational modulation of slow skeletal muscle troponin T by an NH(2)-terminal metal-binding extension. *Am. J. Physiol. Cell Physiol.*, **279**, C1067–C1077.
45. Feng, H.Z., Chen, M., Weinstein, L.S. and Jin, J.P. (2011) Improved fatigue resistance in Gsalpha-deficient and aging mouse skeletal muscles due to adaptive increases in slow fibers. *J. Appl. Physiol. (1985)*, **111**, 834–843.